International Journal of Nanoelectronics and Materials
IJNeaM
ISSN 1985-5761 | E-ISSN 2232-1535

Mathematical modeling of a SiGe HBT: Effect of Ge profiles

Vishal Sharma [a]*, Amit Chaudhry [a]

[a]*Department of ECE, University Institute of Engineering and Technology, Panjab University, Chandigarh 160014, India*
** Corresponding author. Tel.: +91-836-064-4211; e-mail: vishaluiet@pu.ac.in*

Received 29 December 2024, Revised 26 February 2025, Accepted 15 April 2025

ABSTRACT

The performance of a silicon-germanium heterojunction bipolar transistor (SiGe HBT) has been studied with three different Ge doping profiles in the base region. These profiles are triangular (graded), trapezoidal (graded and box combination), and box (constant). The parameters studied are current gain (β), early voltage (Va), βVa, cutoff frequency (fT), and maximum frequency of oscillation (fmax). Additional effects such as temperature, base pushout, low collector current injection effect, bandgap narrowing, and collector voltage variations have been included in the model. The modeled results show that in box profile, β, and emitter delay (τe) are highly improved whereas in the triangular profile, the parameters Va, βVa, and base transit time are highly improved. The trapezoidal approach has intermediate results between the other two approaches. The f_T and fmax are highly improved as compared to Si BJT in all the three cases. The results obtained from the developed model show good agreement with the existing reported results.

Keywords: *Band gap, Collector current, Germanium, Grading, Kirk effect, Early effect*

1. INTRODUCTION

The first homojunction germanium (Ge) bipolar junction transistor (BJT) was designed by Bardeen and Brattain at Bell labs, USA in late 1947 and reported in 1948 [1]. Due to enhanced leakage currents, it showed poor response at high temperatures. The silicon BJT was subsequently designed in 1954 [2]. The development in metal-oxide-semiconductor (MOS) technology was also going on in parallel. However, the BJT had its own advantages such as their use in logic devices and high frequency use in analog circuits. They had also been used with MOS technology such as bipolar complementary MOS (BiCMOS) circuits making use of advantages of both the technologies for wider applications in analog and mixed signal design.

Due to its potential advantages, the BJT was gradually improved in performance, especially in the frequency of operation and current gain. The performance of a BJT can only be improved if its parameters such as base width and doping needed to be decreased to decrease the overall base transit time across the transistor. But this had its own disadvantages such as increase of base resistance and difficulty in realizing extremely small bases in the region of nanometers. Increase of base resistance would reduce the fmax which is discussed in section IV. To further improve the performance beyond the physical limits of the BJT, Kroemer developed the theory of the silicon-germanium heterojunction bipolar transistor (SiGe HBT) in 1957. This technology used two different bandgap semiconductor materials [3]. The use of SiGe HBT helped in improving the BJT high frequency performance using the third degree of freedom by introducing Ge in the base of the transistor instead of reducing the base width and base doping. Though the concept of HBT was proposed in 1957, its actual production started in 1980s [4]. The historical development of the SiGe HBT is detailed in Table 1.

Subsequently, over the last many years, a lot of development has taken place in the field of high frequency operation of SiGe HBTs due to the advances in the field of telephony and mobile communication. These have higher speed performance and higher cut-off frequency as compared to the Si BJT [5]. Besides this, BiCMOS technology has also been used with the combination of both SiGe HBT and CMOS technology. This has opened wide applications in analog, RF, and digital applications domains [6]. Lastly, SiGe HBTs can also be operated in under exposure to intense space radiations and extreme temperatures [7] making them the potential semiconductor devices for the future space research and exploration.

The progress of the high frequency transistors is only possible if the basic understanding of the physical

Table 1. SiGe HBT Development [5]

Year	Development in SiGe HBT
1957	Basic HBT theory
1975	SiGe strained layers
1985	SiGe thin film by MBE
1986	SiGe thin film using CVD
1987	SiGe HBT
1992	SiGe HBT BiCMOS technology
1993	Peak cutoff frequency realized above 100 GHz
2001	Peak cutoff frequency realized above 200 GHz

phenomenon is clear and developed continuously in an analytical manner. The work done in theoretical modeling of the SiGe HBT over the past five decades mainly dealt with either numerical models [8–12] or the empirical models [13, 14] or actual experimentation [15–21] explaining very little about the underlying physics of the device. However, very few works have been done to model the device analytically [22–26]. The empirical models are highly inaccurate and are applicable for a particular set of device parameters. The numerical models are highly mathematically complex.

In this paper, an analytical model the SiGe HBT has been developed when the three Ge profiles namely box profile, triangular profile, and trapezoidal profiles are used in the base of a SiGe HBT. The organization of the paper is described below:

In section II, the physics of strain produced in the Si film due to germanium doping has been dealt with. Section III details the electrical characteristics and parameters of a Si BJT. Section IV gives the physics and modeling of a SiGe HBT for three different Ge profiles. The results and discussions on the above model are given in Section V. Section VI concludes the paper.

2. PHYSICS OF STRAINED SIGE LAYERS

Si and Ge semiconductors have indirect energy bandgap containing conduction and valence bands. The conduction energy level of Si contains 6 valleys equal in energy and dispersed in 3 dimensions. When the strain is applied, 6 energy valleys are split into 2 out of plane energy valleys and 4 in-plane energy valleys. The 4-fold valleys move downward in energy, resulting in a small reduction in conduction band. The 2-fold valleys move upward in energy as shown in Figure 1 (a). The valence band has heavy holes, light holes, and split off holes' valleys. Similarly, under strain, the valence band degeneracy also gets lifted. The heavy-hole valence band energy valley gains energy, and the light-hole and split-off valence band energy valleys reduce in energy. The results of the application of strain on the conduction bands and valence bands lead to the alteration of these bands resulting in the alteration of the electrical properties of the SiGe layers. The alteration of band structure provides lower effective mass to the charge carriers. The intervalley scattering also gets suppressed. These factors combined together raise the mobility of the charge carriers. The density of states in the case of SiGe layers is also reduced as compared to the Si layers due to the changes in the band structure and the alteration of effective mass of charge carriers. Mathematically, carrier mobility:

$$\mu = q\,\tau/m^* \quad (1)$$

$$v = \mu \cdot E \quad (2)$$

where

$1/\tau$ = Scattering rate
m^* = Effective mass

3. BJT MODELING INCLUDING KIRK AND LOW INJECTION EFFECTS

The Si BJT Schematic is presented in Figure 2.

The current gain (β) in Si BJT [27] is given by Equation (3):

$$\beta si = I_c/I_b \quad (3)$$

where

I_c = Collector current in Si BJT
I_b = Base current in Si BJT

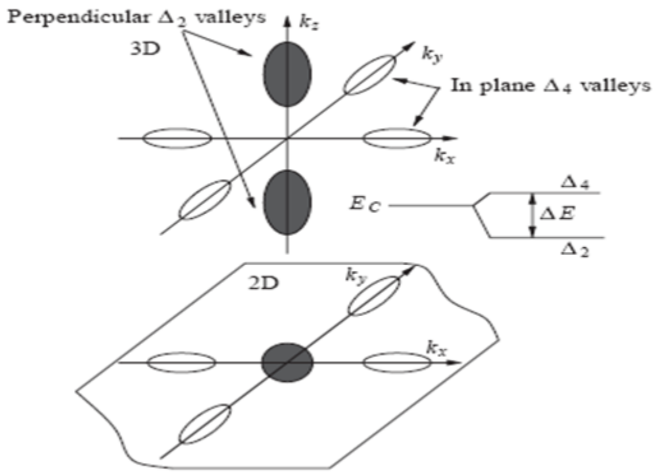

(a)

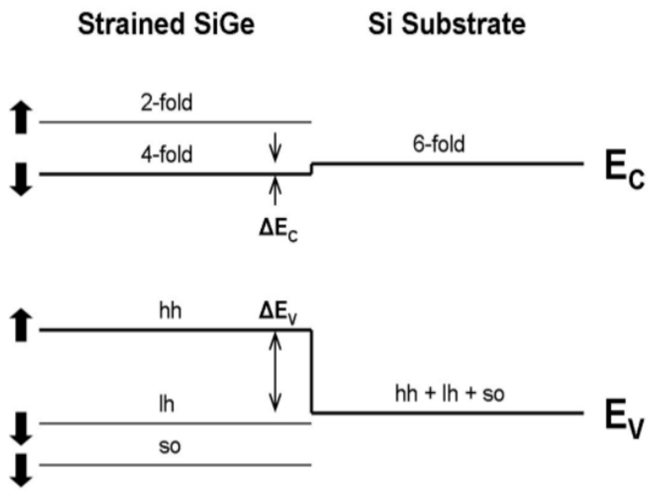

(b)

Figure 1. (a) Conduction band splitting in the presence of strain and (b) resultant bandgap in the SiGe layer after strain [5]

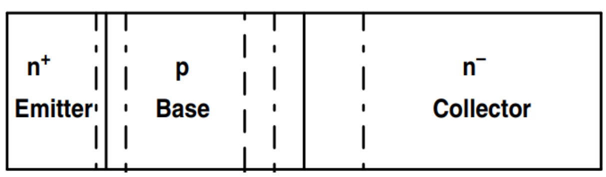

Figure 2. The NPN BJT schematic

The collector current [27] is given by Equation (4):

$$I_c = (qAD_n n_i^2/W_b N_a)\exp\{qV_{be}/kT\} \quad (4)$$

where

q = Electron charge
A = Area of cross-section
D_{nb} = Electron diffusion coefficient in the base
n_i = Intrinsic carrier concentration
W_b = Neutral base width
N_a = Base doping concentration
V_{be} = Biasing voltage at the base
k = Boltzmann constant
T = Absolute temperature

The base current [27] is given by Equation (5):

$$I_b = (qAD_p n_i^2/W_e N_{de})\exp\{qV_{be}/kT\} \quad (5)$$

where

D_{pe} = Hole diffusion coefficient in emitter
W_e = Neutral emitter width
N_{de} = Emitter doping concentration

Therefore, the current gain (β) for a Si BJT is given by Equation (6):

$$\beta si = (D_{nb}W_eN_{de})/(D_pW_bN_a) \quad (6)$$

Equation (6) does not include second order effects such as Kirk effect and low collector current gain degradation. The parameters are defined in Table 2.

3.1. Effect or Base Pushout Effect

Kirk effect is a very important concept in understanding the working of the BJT at high base to emitter voltages in a common emitter configuration. In this concept, the base region is widened, when high collector currents pass through the BJT collector region. Hence the electron density (in case of NPN BJT) increases in the base/collector depletion region. This results in the spread of the electric field in the collector region to balance the electric field in the base region due to enhanced electron density. This process goes on till the whole collector region is covered up and the whole collector region is depleted. If the collector current increases further, there is a collapse of electric field in the collector, and the little electric field exists at the end of the collector region. So, effectively, the base of the transistor gets effectively widened leading to decrease in the β of the BJT. This is due to the fact that electrons take more time in transiting the base region and hence less collector current is produced. The collector current (I_{ckirk}) which is mainly drift current at the start of kirk effect [27] is given by Equation (7):

$$I_{ckirk} = AN_{dc}v_{sat}q \quad (7)$$

where

N_{dc} = Collector region doping
v_{sat} = Electron drift velocity

The parameters used in modeling are given in Table 2. The base width widening (W_{bkirk}) has been taken from [28] and reproduced here as in Equation (8):

$$W_{bkirk} = W_b[1-(x_d/W_b)/(1+I_c/I_{ckirk})^{1/2}] \quad (8)$$

where x_d is the base collector junction depletion width [28] at a collector voltage (V_{cb}).

So, replacing the base width W_b in (6) with W_{bkirk} form (8), we get current gain at high collector current (βsi_1) given by Equation (9):

$$\beta si_1 = (D_{nb}W_eN_{de})/(D_pW_{bkirk}N_a) \quad (9)$$

So, Equation (9) becomes Equation (10) after using Equation (6) as:

$$\beta si_1 = \beta si W_b/W_{bkirk} \quad (10)$$

3.2. Low Collector Current Gain Degradation

The current gain of a BJT also falls at low collector current levels. This is due to the fact that the base current mainly consists of the diffusion currents (5). The generation and

Table 2. Parameters used in development of model

Parameter	Value
Ge in SiGe base	0–0.3
η [27]	1.20
γ	0.25
A	1×10^{-8} cm^2
ξ	0, 0.5, 0.88, 1
ΔEg,Ge(0)	2%, 4%
W_b	1×10^{-5} cm and 5×10^{-6} cm
W_e	1×10^{-4} cm, 5×10^{-4} cm
N_b	1×10^{18} cm^{-3}, 3.3×10^{18} cm^{-3}, 6.6×10^{18} cm^{-3}
N_{de}	8×10^{18} cm^{-3}, 2.6×10^{18} cm^{-3}, 5.2×10^{18} cm^{-3}
R_c [27]	91 Ω
R_b [31]	25 Ω

Parameter	Value
N_{dc}	1×10^{16} cm^{-3}
C_{jc} [27]	19.9 fF
C_{je} [27]	11.7 fF
X_d or W_{cd}	0.69×10^{-5} for V_{bc} = 2V
D_n [28]	30
D_p [28]	45
$n_{i\ silicon}$ [29]	10^{10} /cm^3
v_{sat}	10^5 cm/s
N_t [30]	1×10^{13} cm^3
σ (Electron capture area) [29]	10^{-14} cm^2
R_e [27]	8.3 Ω

recombination currents are also dominant at low collector current levels, and hence the β falls at low base to emitter voltages too ($V_{be} < 0.7$ V).

The whole current gain variation with the base emitter voltage is divided into two parts. The base current at high collector current is mainly diffusive and at low collector current, it is generation and recombination.

For low collector currents, the current gain (β_{si2}) is given by Equation (11):

$$\beta si_2 = I_c/I_{brg} \quad (11)$$

where I_{brg} is the base current [30] at low collector currents given by Equation (12):

$$I_{brg} = 0.5qA\, v_{sat} W_b N_t\, \sigma\, \exp\{qV_{be}/1.76kT\} \quad (12)$$

where

$N_t = 1{\times}10^{13}$ cm^3
σ = Electron capture area (10^{-14} cm^2) [30]

Therefore, the current gain in whole region of operation is the combination of both Equations (10) and (11) in their respective regions as shown in Figure 3.

3.3. Early Voltage (V_A)

The base width modulation (V_A) is a very important and critical parameter for judging the performance of a BJT. The early effect also called as base width modulation is the reduction in effective base width due to the increased base to collector voltage at constant base to emitter voltage [32]. The large collector reverse bias increases the depletion width at the base/collector junction. This leads to the reduction in the base recombination current and hence the collector current starts increasing with the increase of collector base voltage. This is an abnormal second order effect in a BJT which must be studied in order to shift to the SiGe HBT modeling. The early voltage of a Si BJT is the extrapolated tangent to the I_c/V_{ce} curve. The larger the slope of the tangent, the smaller the early voltage. Or the smaller the slope, (lesser value of conductance produced due to early effect), the larger will be the early voltage. So, the early effect voltage must be increased so that the transistor does not produce any change in collector current with the change in base collector voltage. The collector current can only be increased with the increase of base to emitter voltage. Idealy the output conductance ($\partial I_c/\partial V_{ce}$ at fixed V_{be}) should be zero or infinite output resistance (slope of I_c/V_{ce} curve are parallel to x axis).

Figure 4 shows that the early voltage for Si BJT ($V_{A,Si}$) is the x intercept of the tangent to the I_c/V_{ce} curve. We define a point $I_c(0)$ and $V_{ce} = V_{be}$ point on the I_c/V_{ce} curve. $V_{ce} = V_{be}$ implies, $V_{cb} = 0$ volt point. Equation of the tangent at this point becomes Equation (13.1):

$$y - I_c(0) = m(x - V_{be}) \quad (13.1)$$

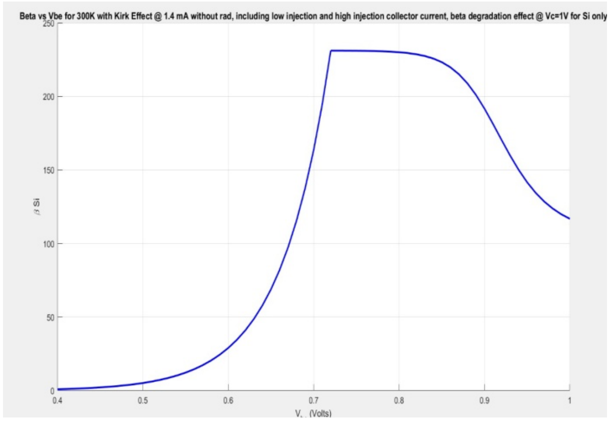

Figure 3. Current gain variation with V_{be} with kirk effect and low injection collector current at collector voltage (Vc) = 1 V for Si BJT

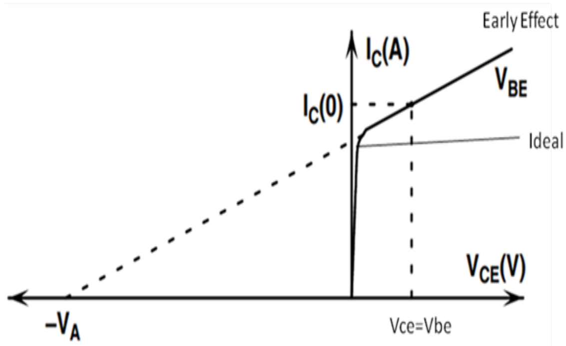

Figure 4. Early voltage of a Si BJT

where $m = \partial I_c/\partial V_{ce}$, so Equation (13.1) becomes $y - Ic(0) = (\partial I_c/\partial V_{ce})\,(x - V_{be})$.

At y = 0, Equation (13.1) becomes Equation (13.2):

$$x = V_{be} - I_c(0)/(\partial I_c/\partial V_{ce}) \quad (13.2)$$

where $x = -V_A$.

Therefore,

$$V_A = V_{be} - I_c(0)/(\partial I_c/\partial V_{ce}) \quad (13.3)$$

Now, Equation (13.3) can be transformed into Equation (13.4) using suitable substitutions [5]:

$$V_{A,Si} = -W_b(0)(\partial W_b/\partial V_{cb})^{-1} \quad (13.4)$$

where $W_b(0)$ is the effective base width at $V_{cb} = 0$ V, and Equation (13.5) can be written as:

$$W_b(V) = W_b - [2\varepsilon_o \varepsilon_{si} N_{dc}(\varphi_{bi} + V_{cb})/(qN_a N_{dc})]^{0.5} \quad (13.5)$$

where

φ_{bi} = Output built-in voltage
ε_o = Permitivity of free space
ε_{si} = Relative permitivity of Si
V_{ce} = Collector-to-emitter voltage
N_{dc} = Doping in collector region

Equation (13.4) can be solved and the final early voltage for a Si BJT can be reached at Equation (13.6):

$$V_{A,Si} = 2(W_b - k_1(\varphi_{bi})^{1/2})(\varphi_{bi}+V_{cb})/k_1 \quad (13.6)$$

where k_1 is equal to $[2\varepsilon_o\varepsilon_{si}N_{dc}/(qN_aN_{dc})]^{0.5}$.

3.4. Base Transit Time ($\tau_{b,Si}$)

It is the time required by the charge carriers (electrons/holes) to cross the base region of a Si BJT after the recombination is over. For Si BJT, it can be easily derived and [27] is given by Equation (14.1):

$$\tau_{b,Si} = W_b^2/2D_{nb} \quad (14.1)$$

The base transit time gets changed if the Kirk effect [28] is taken into account. The changed in Equation (14.2) is given by:

$$\tau_{b,Si} = (W_b^2/2D_{nb})[1-(x_d/W_b)/(1+I_c/I_{ckirk})^{1/2}]^2 + W_b/v_{sat}(1-(x_d/W_b)/(1+I_c/I_{ckirk})^{1/2}] \quad (14.2)$$

3.5. Emitter Delay ($\tau_{e,Si}$)

It is the delay caused by the charge carriers to cross the emitter region. For Si BJT, it can be easily derived and [27] is given by Equation (14.3):

$$\tau_{e,Si} = W_eW_bN_a/2N_{de}D_{nb} \quad (14.3)$$

The parameter values are given in Table 2.

4. SIGE HBT WITH THREE GE PROFILES

A SiGe HBT contains a SiGe base and Si emitter and a Si collector. The addition of Ge with Si in the base region reduces the bandgap as compared to that of Si-BJT. The bandgap of Ge is 0.67 eV. It is lower than the bandgap of silicon (1.11 eV) [29].

4.1. Principle of Addition of Ge in the Base for Three Profiles

The germanium addition in silicon base is not a simple procedure. We are taking here uniform base p type doping of around 1×10^{18} cm^{-3}. The Ge added results in the grading of the conduction band edge as shown in Figure 5. The germanium is added such that the total area covered by each profile is equal. For example, if area covered by triangular profile is "a" units then the area of the trapezoidal profile is also "a" units and vice versa as shown in Figure 6.

Suppose we take $\Delta E_{g,Ge}(0)$ (reduction of bandgap due to addition of Ge at the base-emitter interface) for 2% Ge for all profiles and ΔE_g(grade) (variation of bandgap of SiGe material along the base axis from emitter to collector due to variation in Germanium in the base) of 5% Ge for box (It is a constant value added to the $\Delta E_{g,Ge}(0)$ in the case of box profile for calculation purpose only. In other profiles, it is actual grading of some variable value). We can find the ΔE_g(grade) for rest of the two profiles by equating the respective areas. The area equalization shows a ΔE_g(grade) of Ge 6.6% for trapezoidal and 10% Ge for triangular profile. This means that to achieve same effect of Ge in the base, we add different maximum values of the germanium concentration. The x_T is normally chosen at the half of W_b. ($x_T = 0.5W_b$). $\xi = X_T/W_b$.

4.2. Relationship between Ge Concentration and the Bandgap Reduction

The Ge concentration added in the Si base causes a reduction of bandgap of Si. It is estimated that for every 10% addition of the Ge in the Si, there is a reduction of bandgap of 75 meV [5]. So, for every 1% Ge addition, 7.5 meV bandgap is reduced. For a Ge addition of 15% in triangular profile, the ΔE_g(grade) = 15×7.5 meV = 112.5 meV. At room temperature, kT = 26 meV. Therefore, ΔE_g(grade)/kT = 112.5/26 = 4.32. If we reduce the temperature to 77 K, then the ratio is 112.5/6.5 = 17.3. The electrical parameters estimation done in this paper are based on these Ge addition principles.

4.3. Current Gain Ratio in Case of Three Ge Profiles

The collector current density for the SiGe HBT can be evaluated using the fundamental Moll and Ross Equation [33, 34] expressed in Equation (15.1). The integral limits are from 0–W_b:

$$I_{Csige} = Aq\{\exp(qV_{be}/kT)-1\}/\int (p_b(x)dx/n_{ib}^2(x)D_{nb} \quad (15.1)$$

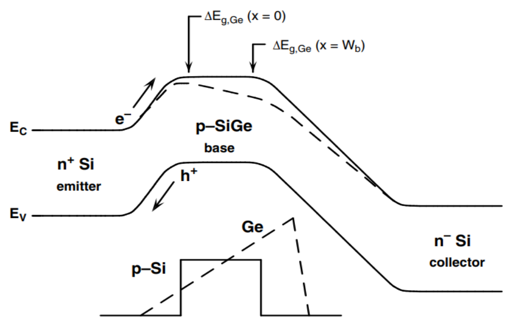

Figure 5. Energy band diagram of a biased SiGe HBT [5]

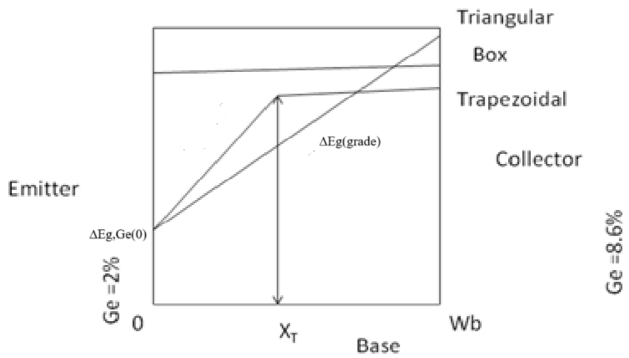

Figure 6. Cross section of HBT with Ge doping profiles in base. The three profiles have been taken

where

$p_b(x)$ = Na = Constant base doping
$n^2_{ib}(x) = (NcNv)_{SiGe}(x)\exp(-E_g(x)/kT)$
Nc = DOS of conduction band
Nv = DOS of valence band for SiGe doped base
E_g = Variable bandgap in the base region of SiGe HBT

When we evaluate Equation (15.1), the final Equation [5] comes out to be Equation (15.2):

$$I_{csige} = A(qD_{nb}/N_{ab}W_b)\exp(qV_{be}/kT - 1)n_{io}^2\exp(\Delta Eg,Ge(0)/kT)(\gamma\eta\exp\Delta Eg(grade))/kT/1-\exp-(\Delta Eg(grade))/kT) \quad (15.2)$$

where

$\Delta E_{G(0)}$ = Energy bandgap reduction at the base/emitter interface due to Ge addition
$\Delta E_{G(Wb)}$ = Energy bandgap reduction at the base/collector interface
$\Delta Eg(grade) = \Delta E_{G(Wb)} - \Delta E_{G(0)}$ is the gradient of Ge along the base
D_{nb} = Electron diffusivity in the base of SiGe
γ ($\gamma < 1$) = Ratio of the product of the density of states of SiGe and Si BJT
η = Ratio of the diffusion coefficients of SiGe and Si BJTs = 1.2

The β ratio of the SiGe and the Si BJT is given in Equation (16):

$$\beta_{sige}/\beta_{si} = A/B \quad (16)$$

where

$A = \gamma\eta\exp(\Delta Eg,Ge(0)/kT$
$B = \xi kT\Delta Eg(grade)+\{1-\xi(1+kT\Delta Eg(grade))\}\exp-\Delta Eg(grade)/Kt$

This is obtained by dividing the collector current density in SiGe HBT from Equation (15.2) with the Si BJT collector current from Equation (4) and as shown in Figures 7 and 8. Figure 7 shows a β variation for SiGe with the base to emitter voltage. It is obtained when Equation (16) is multiplied with Equation (9) and Equation (11). Figure 8 shows the current gain ratio in case of SiGe and Si with the temperature. The collector current ratio is approximately same as that of the current gain ratio as the common factor is the base current. The base current is same in both the cases of SiGe HBT and Si BJT.

4.4. Early Voltage for Three Profiles ($V_{a,SiGe}$)

The early effect in a BJT has been discussed in detail in previous section. The early voltage enhancement [5] in the case of SiGe HBT is expressed in Equation (17) as shown in Figure 9.

$$V_{a,SiGe}/V_{a,Si} = E/F \quad (17)$$

where

$E = 1-\xi+\xi(\exp\Delta Eg(grade)/kT-1)$
$F = \Delta Eg(grade)/kT$
$\xi = x_T/W_b$

The (βV_a) is given in Figure 10.

4.5. Forward Transit Time (τ_f)

Equation (18) represents the forward transit time. Its components are τ_e, the emitter delay, the base transit time (τ_B) and the (τ_{cbd}). τ_{ebd} is negligible and can be ignored.

$$\tau_F = \tau_e+\tau_{ebd}+\tau_b+\tau_{cbd} \quad (18)$$

4.6. Base Transit Time (τ_b)

When the Ge is doped into the base of a SiGe HBT in the grading manner such as in triangular profile or the trapezoidal profile, an additional accelerating electric field is created in the base region which pushes the injected

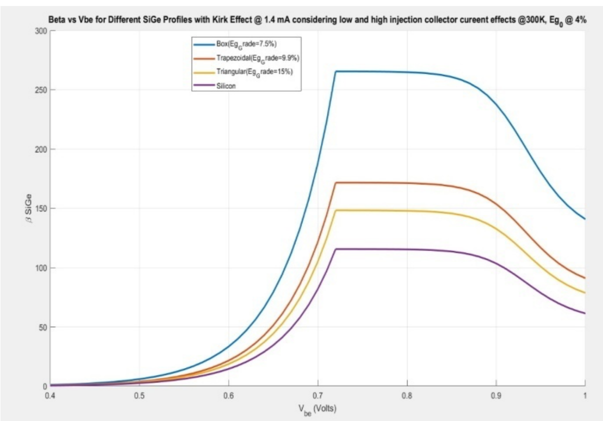

Figure 7. Current gain variation with Vbe with kirk effect and low injection collector current at Vc = 1 V for SiGe HBT. ΔEg,Ge(0) = 4% Ge and ΔEg(grade) = 7.5%, 9.9%, and 15% Ge for box, trapezoidal, and triangular profiles. The modeled results match very well with the reported results [35]

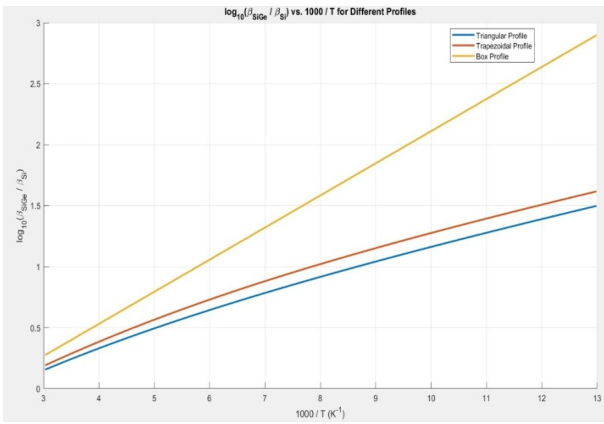

Figure 8. β ratio for SiGe HBT and Si BJT with temperature. ΔEg,Ge(0) = 2% Ge and ΔEg(grade) = 5%, 6.6%, and 10% Ge for box, trapezoidal, and triangular profiles. The modeled results match very well with the reported results [5]

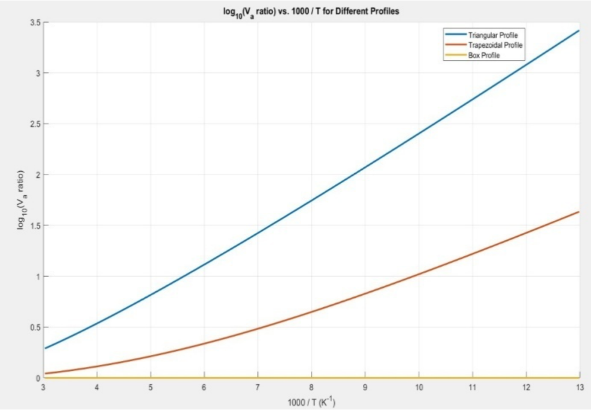

Figure 9. Early voltage ratio ($V_{a\,SIGE}/V_{a\,Si}$) variation with temperature. ΔEg,Ge(0) = 2% Ge and ΔEg(grade) = 5%, 6.6%, and 10% Ge for box, trapezoidal, and triangular profiles. The modeled results match very well with the reported results [5, 36]

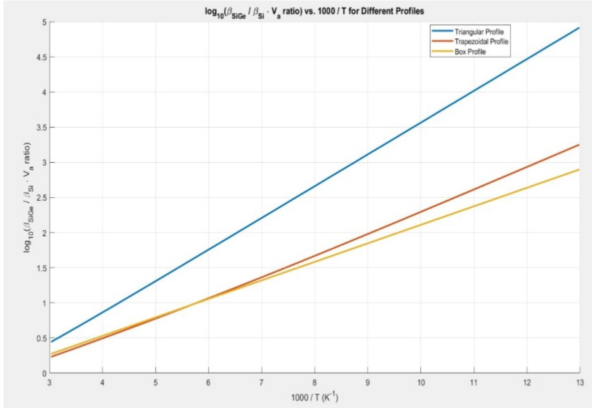

Figure 10. βV_a ratio with temperature. ΔEg,Ge(0) = 2% Ge and ΔEg(grade) = 5%, 6.6%, and 10% Ge for box, trapezoidal, and triangular profiles. The modeled results match very well with the reported results [5, 36]

electrons from emitter to the collector. This phenomenon speeds up the electron movement and hence the base transit time is reduced. If in a triangular profile, we add 5% Ge and hence it is observed that the ΔEg(grade) becomes 38 meV. For a base width W_b of 1x10^{-5}cm, the electric field approximately produced is 3.8 kV/cm. This high field helps additionally in transporting the electrons through the base of the transistor. This would also help in improving the frequency response of the HBT too. The reduction in base transit time τ_b [5] due to Ge addition is given in Equation (19):

$$\tau_{b,SiGe}/\tau_{b,Si} = \{2kT\xi^2/\eta\Delta Eg(grade)\}[\{1/\xi-1-kT/\Delta Eg(grade)\}\{1-\exp-\Delta E(grade)/kT\}+1+\Delta Eg(grade)/2kT(1/\xi-1)^2 \quad (19)$$

The results are shown in Figure 11.

4.7. Emitter Transit Time (τ_e)

The emitter charge storage time (τ_e) [5] in a SiGe HBT can be expressed as Equation (20) and shown in Figure 12:

$$\tau_{e,SiGe}/\tau_{e,Si} = C/D \quad (20)$$

where

$$C = \xi kT/\Delta Eg(grade)+\{1-\xi(1+kT/\Delta Eg(grade)\}\exp(-\Delta Eg(grade)/kT)$$
$$D = \gamma\eta\exp(\Delta Eg,Ge(0)/Kt$$

4.8. Base-to-Collector Transit Time (τ_{cbd})

$$\tau_{cbd} = W_{cb}/2v_{sat} \quad (21)$$

where

W_{cb} = Base-to-collector depletion width
v_{sat} = Electron saturation velocity

The values are given in Table 2.

4.9. Cut-off Frequency (f_T)

f_T is a very critical parameter in evaluating the performance of a SiGe HBT at high frequencies. We know that at high frequencies the current gain (β) starts falling due to the negative feedback caused by the inter electrode

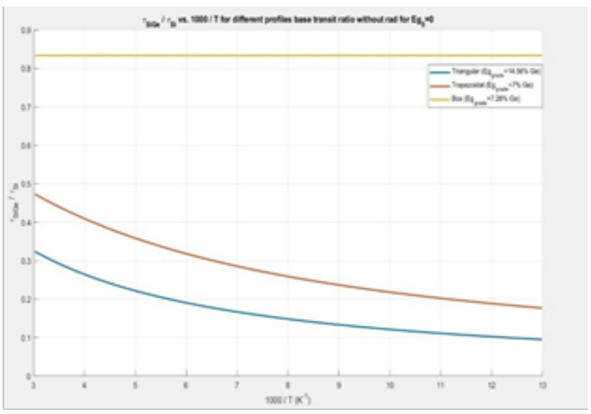

Figure 11. Base transit time ratio with temperature for SiGe HBT. ΔEg,Ge(0) = 0% Ge and ΔEg(grade) = 7.28%, 7%, and 15.56% Ge for box, trapezoidal, and triangular profiles

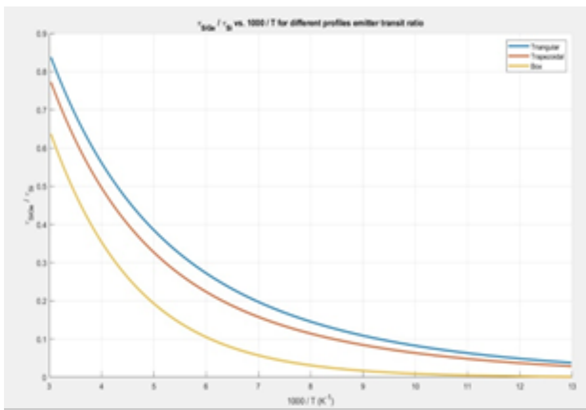

Figure 12. Emitter time ratio (SiGe HBT) variation with temperature for different profiles. ΔEg,Ge(0) = 2% Ge and ΔEg(grade) = 5%, 6.6%, and 10% Ge for box, trapezoidal, and triangular profiles

capacitances. These are base/collector, base/emitter, and emitter/collector. The current gain goes on falling and reaches a point, where it becomes unity. This frequency of operation is called as f_T. Beyond this frequency, we cannot operate the HBT as it becomes useless to operate a transistor with gain less than one. The f_T [27] is dependent on the material and device parameters of a SiGe HBT given in Equation (22).

$$1/2\pi f_T = \tau_f+(R_c+R_e)C_{jc}+kT(C_{je}+C_{jc})/qI_c \quad (22)$$

where

C_{JE} = Emitter-base junction capacitance
C_{JC} = Base-collector junction capacitance
τ_f = Forward transit time

The Equation (22) is derived using the high frequency equivalent circuit of a SiGe HBT. If we examine the Equation (22), it is easily seen that the f_T is directly the function of collector current. As the collector current increases till the Kirk limit, the f_T will go on increasing (Figure 13). The rise in collector current means that the base transit time will fall. This is only possible if the Ge is added in the base with the grading technique. If the Ic is low, then the f_T is also very low. After the Kirk limit, the increase of Ic leads to the decrease in the f_T as the base transit time starts increasing due to the base widening effect. The base transit time and emitter delay are a function of Ge doping in the base and determine the f_T of a SiGe HBT. The Equation (22) is evaluated using Equations (14.1), (14.2), (14.3), (19), (20) and (21).

4.10. Maximum Frequency of Oscillation (f_{max})

It is the value of the frequency at which the power gain (G) of a SiGe HBT drops to unity. The power gain of SiGe HBT [37] given in Equation (23.1) (Figure 14):

$$G^2 = (f/f_{max})^2 \quad (23.1)$$

For unity power gain, it is found that the operating frequency is given by f_{max} [27]as given in Equation (23.2):

$$f_{max} = (f_T/8\pi C_{jc}R_b)^{1/2} \quad (23.2)$$

where

C_{JC} = Base-to-collector junction capacitance
R_b = Base resistance

Equation (23.2) is evaluated using Equation (22) and parameters from Table 2.

5. RESULTS AND DISCUSSION

We have analytically modeled the working of the SiGe HBT when three types of Ge profiles are used in the silicon base of the NPN BJT. The current gain of a BJT has always been assumed to be constant. But as we include the second order effects, the results become different. The results in Figure 3

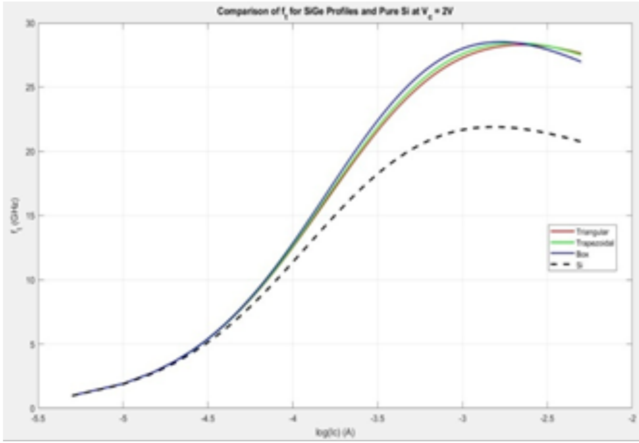

Figure 13. f_T variation with Ic with kirk effect at Vc = 2 V for SiGe HBT. ΔEg,Ge(0) = 2% Ge and ΔEg(grade) = 5%, 6.6%, and 10% Ge for box, trapezoidal, and triangular profiles. The modeled results match very well with the reported results [11]

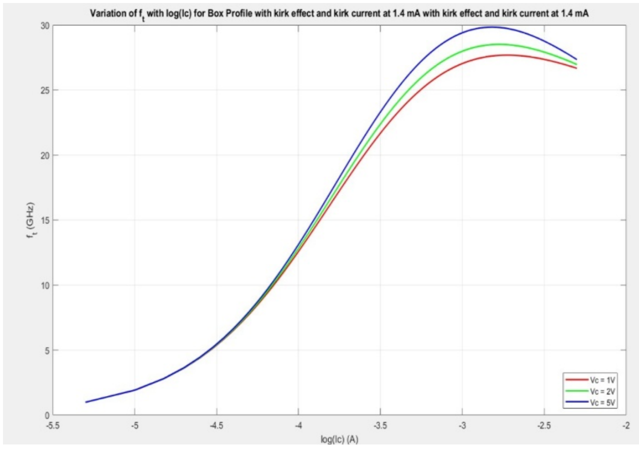

Figure 14. f_T variation with Ic with kirk effect at Vc = 1 V, 2 V, and 5 V for SiGe HBT. ΔEg,Ge(0) = 2% Ge and ΔEg(grade) = 5%, Ge for box profiles

clearly show that Kirk effect and the low collector currents, reduce the current gain for a Si BJT.

Figure 16 shows the variation of Ge across the base of the SiGe HBT. The three profiles generated have ΔEg,Ge(0) (a constant factor at the base/emitter interface). This factor is usually 2% of Ge in the base. The calculations show that for every 1% added Ge in Silicon, the bandgap of Si falls by 7.5 meV. For 2% Ge, the band reduction is 15 meV. So, at the base/emitter interface, the fall in energy bandgap is 15 meV. As we move from base/emitter interface to base/collector interface, it is seen that there are three paths. One is the constant path. This path is called box profile due to the shape of the rectangular box in the base. The bandgap of Si has been reduced constantly from one interface to the other. This reduction in bandgap across the base is called as ΔEg(grade). So, total bandgap reduction is the ΔEg,Ge(0)+ ΔEg(grade)(box) in case of box profile.

In the second profile, the path goes from ΔEg,Ge(0) to the other end of the base/collector interface. This is called triangular profile. In this profile, the Ge concentration varies from ΔEg,Ge(0) at the base/emitter interface to Eg(Wb) at the base/collector interface. The net change in energy bandgap is called ΔEg(grade)(triangular) = (Eg(W_b)–ΔEg,Ge(0)).

The third path is called trapezoidal profile. It starts from the base-emitter interface and reaches at the peak in the middle of the base or any point desired in the base (x_T) where the Ge concentration peaks. After that, it follows a constant pattern as box profile. So, it has two variations. One is the triangular profile, and the other is the box profile. So, the combination of these two profiles yields a full model of the trapezoidal profile. Figure 7 shows current gain variation with V_{be} with Kirk effect and low injection collector current at Vc = 1 V for SiGe BJT. ΔEg,Ge(0) = 4% Ge and ΔEg(grade) = 7.5%, 9.9%, and 15% Ge for box, trapezoidal, and triangular profiles. These curves show that the "β" is very high for the box profile and very low for the triangular profile. The trapezoidal profile shows an intermediate effect in the whole simulation of the current gain. The possible reasons for such behavior are the dependence of the collector current ratio in two cases of SiGe HBT and the Si BJT on the Ge profile in the base region. If the Ge content in the base is constant, then the collector current increases exponentially and not linearly across the base. The exponential increase is very fast and larger than linear and hence the box profile dominates in the overall gain enhancement. This can be explained clearly using Equation (16) by evaluating it for three profiles.

For box profile (ξ = 0), it reduces to β_{sige}/β_{si} = γη exp (ΔEg(grade)(box)+ΔEg,Ge(0)/kT). This expression clearly shows that gain enhancement of box is exponentially dependent on the Ge induced bandgap net reduction. For triangular profile, (ξ = 1), β_{sige}/β_{si} = (γη/kT) (ΔEg(grade)(triangular)) exp(ΔEg,Ge(0)/kT). Dividing gain enhancement box with triangular, we get approximately exp(ΔEg(grade)(box)/ΔEg(grade)(triangular). It clearly shows that gain enhancement of box profile is more than the triangular profile. Due to the linearity in the gain enhancement of triangular profile, it is at the 3rd position than the exponential box profile.

For trapezoidal profile, the results are mixed having impact of both box and triangular profiles and comes at 2nd place. The Si BJT comes at 4th position, the lowest in the gain out of 4. Figure 9 shows the variation of early voltage ratio (V_{asige}/V_{asi}) with the temperature. As the temperature falls from 300 K to 77 K, there is a sharp increase in the early voltage ratio for triangular and trapezoidal profiles. For box profile (ξ = 0), it reduces to V_{asige}/V_{asi} = 1. There is no effect of temperature on the box profile. Early voltage enhancement increases more for triangular and less for trapezoidal as the temperature falls. For triangular profile, (ξ = 1), Va_{sige}/Va_{si} = kT (exp (ΔEg(grade)(triangular)/kT)–1) / ΔEg (grade) (triangular). For trapezoidal profile, (ξ = 0.5), Va_{sige}/Va_{si} = 0.5 + 0.5kT (exp(ΔEg(grade)(trapezoidal)/kT)–1)/ΔEg(grade)(trapezoidal). If we take the ratio of both the equations, it is found that the triangular profile early voltage enhancement is approximately double that of the trapezoidal profile. This analysis explains the results obtained.

Figure 10 explains the figure of merit of the SiGe HBT i.e., gain early voltage product ratio. For box profile (ξ = 0), it reduces to $\beta Va_{sige}/\beta Va_{si}$ = γη exp(ΔEg(grade)(box)+ ΔEg,Ge(0)/kT). This expression clearly shows that gain Va enhancement of box is exponentially dependent on the Ge induced bandgap net reduction. For triangular profile, (ξ = 1), $\beta Va_{sige}/\beta Va_{si}$ = (γη)exp(ΔEg(grade)(triangular)+ ΔEg,Ge(0)/kT). Dividing both box and triangular expressions, we get the value (γη)exp(ΔEg(grade) (triangular)–ΔEg(grade)(box)/kT). This expression is greater than unity because the ΔEg(grade) of triangular profile (10%) is more than box profile (5%). So, the FOM of triangular profile is the maximum and box is the minimum and trapezoidal is in between the two.

Figure 11 shows base transit time ratio with temperature for SiGe HBT. ΔEg,Ge(0) = 0% Ge and ΔEg(grade) = 7.28%, 7%, and 15.56% Ge for box, trapezoidal, and triangular profiles, respectively. For box profile (ξ = 0), the ratio is 1/η which is a constant factor. So, the base transit times are constant and for SiGe HBT it is little lesser than the Si BJT.

For (ξ = 1), the base time ratio becomes 2kT/(ηΔEg(grade)). Therefore, it clearly shows that for high or sharp ΔEg(grade), the base transit time falls very rapidly as also shown in the Figure 10. The trapezoidal curve is in between the box and the triangular profile. Clearly, the triangular profile is much better here. At 300 K, the τ_b, ratio is around 1.3 for triangular profile which is the least out of the three profiles.

Figure 13 shows f_T variation with Ic with kirk effect at Vc = 2V for SiGe HBT. ΔEg,Ge(0) = 2% Ge and ΔEg(grade) = 5%, 6.6%, and 10% Ge for box, trapezoidal, and triangular profiles. It shows that all the profiles generate higher f_T than the Si BJT. Figure 15 shows f_{max} variation with Ic with kirk effect at Vc = 1 V for all three profiles and Si BJT. The results show that the f_{max} in SiGe HBT is highly improved than the Si BJT. Figure 16 shows fmax and f_T variation with Ic with kirk effect at Vc = 1 V for three profiles ΔEg,Ge(0) = 2% Ge and ΔEg(grade) = 5%, 6.6%, and 10% Ge for box, trapezoidal, and triangular profiles. It is clear from the figure that the f_{max} is nearly double (45 GHz) than the f_T (28 GHz) for all the profiles. Clearly, all three profiles are better than the Si BJT (f_{max} = 40 GHz and f_T = 23 GHz) and hence the justification of the modeled results have been established.

6. CONCLUSION

SiGe HBT development has been going on due to its potential applications in many niche areas and in future, it may become a main prime mover to run the microelectronic industry in some of the extreme engineering areas such as space exploration and cryogenics. A systematic, physics based and simple to understand approach has been used to analytically model the performance of a SiGe HBT with three different Ge base doping profiles. The parameters studied are β, Va, βVa, f_T, and f_{max}. The additional effects such as temperature, kirk effect, low collector current injection effect, bandgap narrowing, early effect, and collector

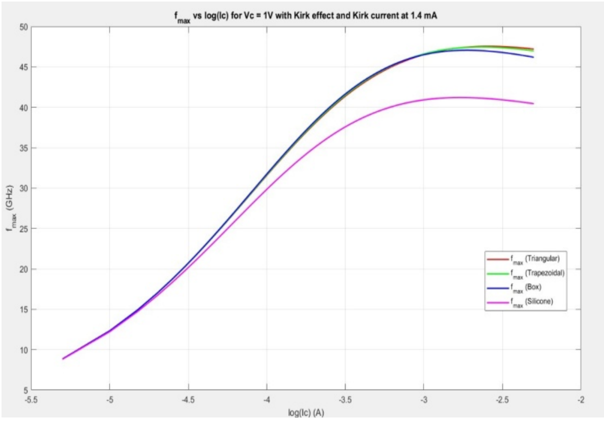

Figure 15. f_{max} variation with I_c with kirk effect at V_c = 1 V, for all box, triangular, and trapezoidal profile SiGe HBT and Si BJT. ΔEg,Ge(0) = 2% Ge and ΔEg(grade) = 5%, 6.6%, and 10% Ge for box, trapezoidal, and triangular profiles

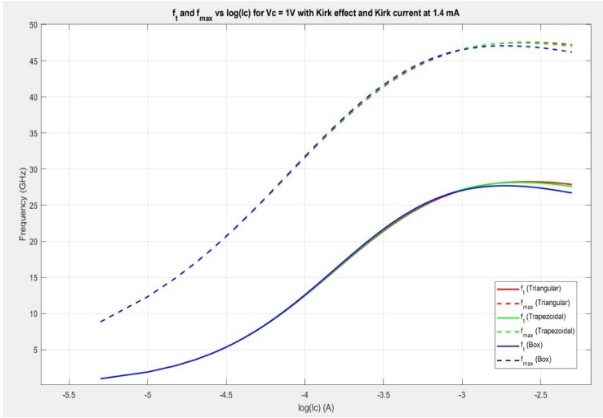

Figure 16. f_{max} and f_T variation with Ic with kirk effect at Vc = 1 V for all three profiles. ΔEg,Ge(0) = 2% Ge and ΔEg(grade) = 5%, 6.6%, and 10% Ge for box, trapezoidal, and triangular profiles

voltage variations have provided a lot of accuracy to the developed model. The methodology to find the actual Ge concentration in all three profiles has been given in the model. The modeled results show that in box profiles β and emitter charge storage time (τ_e) are highly improved whereas in the triangular profile, the parameters Va and βVa, base transit time are highly improved. The trapezoidal approach has intermediate results between the other two approaches. The trapezoidal profile calculation can be further improved by taking the x_T point at other places in the base region. The f_T and f_{max} are highly improved as compared to Si BJT in all the three cases. The results obtained from the developed model show good agreement with the existing reported results. Further investigations using effects such as radiation effects, noise, neutral base recombination effect and non-uniform base doping can also be studied analytically.

ACKNOWLEDGMENTS

The authors express their gratitude to all the individuals and fellow colleagues of the UIET, Panjab University, Chandigarh, India for motivating us. Our special thanks go to Ms. Kannu Mittal, M.Tech student (Pass out), and Nikhil Dubey and Saksham Shukla, current students of UIET for assisting in coding for the above work.

REFERENCES

[1] J. Bardeen and W. H. Brattain, "The Transistor, A Semi-Conductor Triode," *Physical Review*, vol. 74, no. 2, pp. 230–231, 1948.

[2] M.Riordan, "The lost history of the transistor," *IEEE Spectrum*, vol. 41, no. 5, pp. 44–49, 2004.

[3] H. Kroemer, "Theory of a Wide-Gap Emitter for Transistors," *Proceedings of the IRE*, vol. 45, no. 11, pp. 1535–1537, 1957.

[4] S. S. Iyer, G. L. Patton, S. S. Delage, S. Tiwari, and J. M. C. Stork, "Silicon-germanium base heterojunction bipolar transistors by molecular beam epitaxy," in *1987 International Electron Devices Meeting*, IRE, 1987, pp. 874–876.

[5] J. Cressler and G. Niu, *Silicon-Germanium Heterojunction Bipolar Transistors*. Artech, 2002.

[6] P. Magnee, D. Leenaerts, M. van der Heijden, T. V. Dinh, I. To, and I. Brunets, "The future of SiGe BiCMOS: bipolar amplifiers for high-performance millimeter-wave applications," in *2021 IEEE BiCMOS and Compound Semiconductor Integrated Circuits and Technology Symposium (BCICTS)*, IEEE, 2021, pp. 1–7.

[7] J. D. Cressler, "The Silicon-Germanium Heterojunction Bipolar Transistor," *IEEE Electron Devices Society Newsletter*, pp. 6–8, 2022.

[8] U. Saha, F. Imteaz, O. P. Saleque, Md. M. H. Shohag, and B. Debnath, "Numerical simulation of Silicon-Germanium Heterojunction Bipolar Transistor (HBT) in silvaco/atlas and analysis of HBT base transit time to achieve faster operation," in *2015 International Conference on Electrical Engineering and Information Communication Technology (ICEEICT)*, IEEE, 2015, pp. 1–4.

[9] K. H. Kwok and C. R. Selvakumar, "Profile design considerations for minimizing base transit time in SiGe HBTs for all levels of injection before onset of Kirk effect," *IEEE Transactions on Electron Devices*, vol. 48, no. 8, pp. 1540–1549, 2001.

[10] D. M. Richey, J. D. Cressler, and A. J. Joseph, "Scaling issues and Ge profile optimization in advanced UHV/CVD SiGe HBT's," *IEEE Transactions on Electron Devices*, vol. 44, no. 3, pp. 431–440, 1997.

[11] G. Zhang, J. D. Cressler, G. Niu, and A. Pinto, "A comparison of npn and pnp profile design tradeoffs for complementary SiGe HBT Technology," *Solid-State Electronics*, vol. 44, no. 11, pp. 1949–1954, 2000.

[12] D. J. Roulston, S. G. Chamberlain, and J. Sehgal, "Simplified computer-aided analysis of double-diffused transistors including two-dimensional high-level effects," *IEEE Transactions on Electron Devices*, vol. 19, no. 6, pp. 809–820, Jun. 1972.

[13] I. Angelov, D. Schreurs, K. Andersson, M. Ferridahl and F. Ingvarson, *34th European Microwave Conference, 2004.*, 2004, pp. 229–232.

[14] C. -I. Lee, Y. -T. Lin, B. -R. Su and W. -C. Lin, "SiGe HBT

Large-Signal Table-Based Model with the Avalanche Breakdown Effect Considered," in *IEEE Transactions on Electron Devices*, vol. 62, no. 1, pp. 75–82, 2015.
[15] Q. Z. Liu *et al.*, "A Self-Aligned Sacrificial Emitter Process for High Performance SiGe HBT in BiCMOS," *ECS Transactions*, vol. 50, no. 9, pp. 121–127, 2013.
[16] J. C. J. Paasschens, W. J. Kloosterman and R. J. Havens, *Proceedings of the 2001 BIPOLAR/ BiCMOS Circuits and Technology Meeting (Cat. No.01CH37212)*, 2001, pp. 38–41.
[17] Z. Matutinovic-Krstelj, V. Venkataraman, E. J. Prinz, J. C. Sturm and C. W. Magee, "Base resistance and effective bandgap reduction in n-p-n Si/$Si_{1-x}Ge_x$/Si HBTs with heavy base doping," in *IEEE Transactions on Electron Devices*, vol. 43, no. 3, pp. 457–466, 1996.
[18] H. Rücker, J. Korn and J. Schmidt, "Operation of sige HBTs at cryogenic temperatures," *2017 IEEE Bipolar/BiCMOS Circuits and Technology Meeting (BCTM)*, 2017, pp. 17–20.
[19] G. Niu *et al.*, "SiGe profile design tradeoffs for RF circuit applications," *International Electron Devices Meeting 1999. Technical Digest (Cat. No.99CH36318)*, 1999, pp. 573–576.
[20] A. J. Joseph, J. D. Cressler, D. M. Richey and G. Niu, "Optimization of SiGe HBTs for operation at high current densities," in *IEEE Transactions on Electron Devices*, vol. 46, no. 7, pp. 1347–1354, July 1999.
[21] A. Joseph *et al.*, "SiGe HBT NPN device optimization for RF power amplifier applications," *2009 IEEE Bipolar/BiCMOS Circuits and Technology Meeting*, 2009, pp. 174–177.
[22] F. Rabbi, Y. Arafat, and M. Ziaur Rahman Khan, "Analytical modelling of Early voltage and Current Gain of $Si_{1-y}Ge_y$ Heterojunction Bipolar Transistor," in *2011 International Conference on Electronic Devices, Systems and Applications (ICEDSA)*, 2011, pp. 53–58.
[23] M. K. Das, N. R. Das, and P. K. Basu, "Effect of Ge content and profile in the SiGe base on the performance of a SiGe/Si heterojunction bipolar transistor," *Microwave and Optical Technology Letters*, vol. 47, no. 3, pp. 247–254, 2005.
[24] S. T. Chang, Y.-H. Liu, M.-H. Lee, S. C. Lu, and M.-J. Tsai, "Optimal Ge profile design for base transit time of Si/SiGe HBTs," *Materials Science in Semiconductor Processing*, vol. 8, no. 1–3, pp. 289–294, 2005.
[25] J. J. Liou and C. S. Ho, "A physical model for the base transit time of advanced bipolar transistors," *Solid-State Electronics*, vol. 38, no. 1, pp. 143–147, 1995.
[26] A. Kashyap and R. K. Chauhan, "Effect of Ge profile design on the performance of an n–p–n SiGe HBT-based analog circuit," *Microelectronics Journal*, vol. 39, no. 12, pp. 1770–1773, 2008.
[27] P. Ashburn, *SiGe Heterojunction Bipolar Transistors*. Wiley, 2003.
[28] C. T. Kirk, "A theory of transistor cutoff frequency (f_T) falloff at high current densities," in *IRE Transactions on Electron Devices*, vol. 9, no. 2, pp. 164–174, 1962.
[29] S. M. Sze, *Physics of Semiconductor Devices*. Wiley, 1981.
[30] P. Ashburn, D. V. Morgan, and M. J. Howes, "A theoretical and experimental study of recombination in silicon p−n junctions," *Solid-State Electronics*, vol. 18, no. 6, pp. 569–577, 1975.
[31] F. Stein, D. Celi, C. Maneux, N. Derrier and P. Chevalier, "Investigation of the base resistance contributions in SiGe HBT devices," *CAS 2013 (International Semiconductor Conference)*, 2013, pp. 311–314.
[32] J. M. Early, "Effects of Space-Charge Layer Widening in Junction Transistors," in *Proceedings of the IRE*, vol. 40, no. 11, pp. 1401–1406, 1952.
[33] J. L. Moll and I. M. Ross, "The Dependence of Transistor Parameters on the Distribution of Base Layer Resistivity," in *Proceedings of the IRE*, vol. 44, no. 1, pp. 72–78, 1956.
[34] H. Kroemer, "Two integral relations pertaining to the electron transport through a bipolar transistor with a nonuniform energy gap in the base region," *Solid-State Electronics*, vol. 28, no. 11, pp. 1101–1103, 1985.
[35] K. O. Petrosyants and M. V. Kozhukhov, "Physical TCAD Model for Proton Radiation Effects in SiGe HBTs," in *IEEE Transactions on Nuclear Science*, vol. 63, no. 4, pp. 2016–2021, 2016.
[36] A. J. Joseph, J. D. Cressler, D. M. Richey, R. C. Jaeger and D. L. Harame, "Neutral base recombination and its influence on the temperature dependence of Early voltage and current gain-Early voltage product in UHV/CVD SiGe heterojunction bipolar transistors," in *IEEE Transactions on Electron Devices*, vol. 44, no. 3, pp. 404–413, 1997.
[37] M. Reisch, *High-Frequency Bipolar Transistors*, vol. 11. Springer, 2003.